JOURNAL OF NEUROTRAUMA 27:1369–1378 (August 2010)

DOI: 10.1089/neu.2010.1321

Noxious Colorectal Distention in Spinalized Rats Reduces Pseudorabies Virus Labeling of Sympathetic Neurons

Hanad Duale,[1,2] Travis S. Lyttle,[1] Bret N. Smith,[2] and Alexander G. Rabchevsky[1,2]

Abstract

The retrograde transsynaptic tracer pseudorabies virus (PRV) has been widely used as a marker for synaptic connectivity in the spinal cord. Notably, the PRV-152 construct expresses enhanced green fluorescent protein (EGFP). We recently reported a significant attenuation of PRV-152 labeling of the intermediolateral cell column (IML) and celiac ganglia after complete T4 spinal cord transection versus sham injury in rats at 96 h after PRV-152 inoculation of the left kidney. Here we found a significant increase in noxious colorectal distention (CRD)-evoked c-Fos expression in spinal cords of injured versus sham rats without PRV infection. In order to assess whether enhancing neuronal activity in spinalized rats might increase PRV-152 labeling, we subjected awake spinalized rats to 1.5 h of intermittent noxious CRD either: (1) just prior to inoculation, or (2) 96 h after inoculation ($n = 3$/group). Equal numbers of spinalized rats in both groups received PRV-152 inoculations without CRD (non-stimulated; $n = 3$/group). At 96 h post-inoculation fixed spinal cords and left celiac ganglionic tissues were assessed for the distribution and quantification of EGFP-labeled cells. The injured cohort that received CRD just prior to PRV injection showed a significant reduction in EGFP-labeled cells in both the IML and left celiac ganglion compared to non-stimulated injured rats. In contrast, the injured cohort that received CRD 96 h after PRV-152 inoculation showed no differences in EGFP-labeled cell numbers in the IML or celiac ganglia versus non-stimulated injured rats. Interestingly, microglia near c-Fos-positive cells after acute CRD appeared more reactive compared to non-stimulated spinalized rats, and activated microglial cells markedly reduce viral transduction and progression following PRV inoculation of the CNS. Hence our results imply that increased CRD-induced c-Fos expression in the injured paradigm, prior to but not after PRV injection, further attenuates PRV-152 uptake, perhaps through changes in neuronal activity and/or innate neuro-immune responses.

Key words: c-Fos; intermediolateral cell column; microglia; pseudorabies virus; retrograde transsynaptic tracer

Introduction

The central nervous system (CNS) is composed of complex networks of synaptically linked neurons. With the development of neurotropic viruses as an alternative to traditional tract tracing tools, our understanding of complex neuronal circuitry, particularly the innervation of thoracic and abdominal viscera, has greatly advanced (Buijs et al., 2003; Cano et al., 2000, 2004; Card et al., 1990; Glatzer et al., 2003; Hadziefendic and Haxhiu, 1999; Jansen et al., 1997; Nadelhaft et al., 1992; Schramm et al., 1993; Standish et al., 1995). Notwithstanding this progress, there is a paucity of knowledge concerning how neurotrauma, particularly spinal cord injury (SCI), affects neuronal circuitry and/or plasticity as demarcated with the use of neurotropic viruses (Bareyre et al., 2004; Duale et al., 2009; Kim et al., 2002; Lane et al., 2008; Pan et al., 2005; Yu et al., 2003).

To address this issue anatomically, we recently used pseudorabies virus (PRV) constructs isogenic with the Bartha strain as markers for synaptic connectivity in central circuits (Card et al., 1993), in order to assess plasticity of the sympathetic and parasympathetic innervation of the kidney and distal colon, respectively, in normal and injured rat spinal cords (Duale et al., 2009). Specifically, the PRV-152 strain expresses the reporter gene for enhanced green fluorescent protein (EGFP; Smith et al., 2000). The exclusively retrograde transport of PRV-152 occurs in synaptically linked chains of neurons, with higher-order structures becoming labeled at later time points (Ch'ng et al., 2007; Pickard et al., 2002; Smith et al., 2000). Additionally, viral replication within neuronal cell bodies allows the virus to be a self-amplifying marker; thus second-, third-, and fourth-order pre-autonomic neurons that regulate a specific visceral target can be labeled within the spinal cord and higher CNS centers of infected animals.

[1]Spinal Cord and Brain Injury Research Center and [2]Department of Physiology, University of Kentucky, Lexington, Kentucky.

Recent studies from our laboratory have shown that SCI leads to aberrant synaptic remodeling that significantly attenuates the uptake and transportation of neurotropic PRV following inoculation into the kidneys (Duale et al., 2009). This reduction in PRV uptake and/or transportation following SCI was evidenced by decreased PRV-labeled cells at both peripheral (celiac ganglia) and central (intermediolateral cell column; IML) locations. The broader implication is that reduced expression of cell receptors required for viral adsorption and entry after SCI may limit the efficacy of transgene expression, at least in kidney-related sympathetic circuits, and potentially mitigate neuroanatomical and/or physiological outcome measures in conjunction with gene therapy.

Based on the collective evidence we speculated that as a result of spinal shock, the observed decrease in PRV uptake and/or transport after SCI may be due to diminished activity of sympathetic preganglionic neurons (SPN) in the IML. Therefore, in order to extend our studies, we tested the hypothesis that application of noxious stimulus (i.e., prolonged, intermittent colorectal distension; CRD) would increase neuronal activity, and thus increase the number of PRV-labeled cells at both peripheral and central locations in injured stimulated (CRD-positive) more than in injured non-stimulated (CRD-negative) animals.

Methods

Animals and spinal surgery

All animal housing conditions, surgical procedures, and postoperative care techniques were conducted according to the University of Kentucky Institutional Animal Care and Use Committee and the National Institutes of Health (NIH) animal care guidelines. Adult female Wistar rats ($\sim$ 200–250 g) were anesthetized with a mixture of ketamine (80 mg/kg IP; Fort Dodge Animal Health, Fort Dodge, IA) and xylazine (10 mg/kg IP; Butler, Columbus, OH). A total of 26 rats were used and divided into injured and sham cohorts as described below. The injured groups received complete T4 spinal cord transection ($n = 21$) with a sterile scalpel blade following T3 vertebra laminectomy, whereas sham animals ($n = 3$) received only T3 laminectomy as previously described (Cameron et al., 2006; Duale et al., 2009; Hou et al., 2008; Hou et al., 2009). Additionally, two T4-transected rats received no further manipulations in order to compare morphologies of activated microglial cells after 2 weeks. See Table 1 for group designations described below for c-Fos and PRV labeling following acute and/or delayed CRD.

We used the T4 level of injury based on the rat model of autonomic dysreflexia following T5 transection as established by Krassioukov and Weaver (1995), who have since routinely injured at the T4 level due to an arteriovenous malformation found at the T4 vertebra in adult female Wistar rats. Moreover, using PRV labeling methods similar to those used in the present study, kidney-related SPN were found to be located predominantly in the IML and the central autonomic nucleus lying dorsal to the central canal of the spinal cord between T5 and L1 of adult rats (Huang and Weiss, 1999). PRV labeling of the kidney has further indicated that renal SPN are organized in a segmental and an intra-segmental manner, with the renal postganglionic neurons projecting topographically (Huang et al., 2002).

After the surgeries were complete, the erector spinae muscles were sutured with 3-0 polyglactin 910 (Ethicon, Sommerfield, NJ), the field was disinfected with povidone-iodine solution (Nova Plus, Irving, TX), and the skin was closed with Michel wound clips (Roboz, Gaithersburg, MD). For postoperative care immediately after surgery, the animals were subcutaneously injected with 20 mL of lactated Ringer's solution (10 mL in each flank; Baxter Healthcare, Deerfield, IL), and 33 mg/kg cephazolin (Apothecon, Bristol-Myers Squibb, Princeton, NJ) and for injured rats, injection twice daily with 10 mL of Ringer's and cephazolin for up to 10 days to maintain hydration and control bladder infection. Buprenorphine (0.035 mg/kg; Reckitt Benckiser, Slough, Berkshire, U.K.) was also administered subcutaneously once after recovery from anesthesia, and twice daily for the next 3 days, to control postoperative pain. Bladders of injured rats were manually expressed twice daily until the bladder-emptying reflex returned at about 10 days post-injury.

Prolonged, intermittent noxious colorectal distention to elicit c-Fos expression

To initiate spinal viscero-sympathetic reflexes in conscious 2-week-injured ($n = 9$) and sham ($n = 3$) rats (Table 1), they were initially placed in a rodent restrainer (Fisher Scientific, Pittsburgh, PA). A latex balloon-tipped catheter (Swan-Ganz; Edwards LifeSciences, Irvine, CA) was then inserted 2 cm inside the rectum, secured to the tail with tape, and left in place until the animals were habituated to both restraint and catheter placement. Following habituation and measurement of baseline blood pressure, the balloon catheter was inflated with 1.5 mL of air for 30 sec of CRD, after which it was deflated for 60 sec. This 90-sec cycle (30 sec on, 60 sec off) was repeated continuously and monitored for 1.5 h (Cameron et al., 2006; Hou et al., 2008). The animals were then euthanatized and perfused for histology.

Table 1. Experimental Design

			PRV			
OX-42 (microglia)	*c-Fos*		*T4Tx-PRV-CRD+ (stimulated)*		*T4Tx-PRV-CRD-(unstimulated)*	
Naive	*Sham + CRD*	*T4Tx + CRD*	*PRV injected 0.5 h post-CRD*	*PRV injected 96 h Post-CRD*	*PRV injected 0.5 h post-mock*	*PRV injected 96 h post-mock*
2	3	9	3	3	3	3

CRD, colorectal distention; PRV, pseudorabies virus; T4Tx, T4-transected.

PRV injections into the kidneys of injured rats following colorectal distention

At 2 weeks post T4-transection, the PRV was injected into the kidneys of another injury cohort (Table 1), either immediately after 1.5 h of CRD, or 96 h after noxious stimulation ($n = 3$/group; stimulated). Alternatively, the PRV was similarly injected into injured rats that had balloon catheters inserted but did not receive CRD ($n = 3$/group; non-stimulated controls). Following CRD or mock sessions, these injury cohorts ($n = 12$) were re-anesthetized with a mixture of ketamine (80 mg/kg IP) and xylazine (10 mg/kg IP), and a laparotomy was performed to expose the abdominal contents. With the aid of a dissecting stereomicrosope, 3 μL of PRV-152 (green; 10^8 pfu/mL) was injected at three sites (1 μL/site) into the left kidney using a 30-gauge Hamilton syringe (Hamilton, Reno, NV). The injections were uniformly placed at sites on the longitudinal midline of the convex surface of the kidney (Duale et al., 2009; Tang et al., 2004). In some cases, PRV-614 (Banfield et al., 2003), which expresses monomeric red fluorescent protein (mRFP1; a generous gift of Roger Tsien) was used similarly. The injection sites were located by dividing the midline into thirds, and injecting at the rostral and caudal end of the middle third. The needle was held in place for 5 minutes and slowly withdrawn under a dry cotton-tipped stick to absorb reflux, followed by lavage of the peritoneal space with sterile saline. The injection sites were each sealed with a drop of tissue adhesive (3M Vetbond™; 3M, St. Paul, MN). Materials that came into contact with PRV during surgery were cleaned with chlorine bleach (0.05%) solution and properly discarded as biohazard materials. The animals were maintained in a biosafety level 2 facility (96 h) until euthanasia prior to perfusion fixation for histology.

Perfusion and tissue processing

In addition to T4 spinal-transected, non-manipulated animals ($n = 2$), following the sessions of intermittent CRD in rats used either for: (1) c-Fos experiments ($n = 12$); (2) PRV inoculation of the kidney immediately following injury ($n = 6$); or (3) PRV inoculation of the kidney at 96 h post-injury ($n = 6$), all rats were overdosed with sodium pentobarbital (150 mg/kg; Abbott, Chicago, IL), and perfused transcardially with 0.1 M phosphate-buffered saline (PBS; pH 7.4), followed by 4% paraformaldehyde in 0.1 M PBS. The spinal cord from the conus medullaris to the transection site was removed, post-fixed for 4 h, rinsed in 0.2 M phosphate buffer (PB) overnight, and cryoprotected for at least 48 h in 20% sucrose in 0.1 M PBS. The caudal and rostral limits of the dissected spinal cords sampled were between 0.5 mm rostral of the conus medullaris ($\sim$ S4) to 6 cm rostral at the T5 segment. The cords were then divided into two 3-cm portions of caudal (S4–T13; lumbosacral) and rostral segments (T12–T5; thoracic), and embedded in gum tragacanth (Sigma-Aldrich, St. Louis, MO) in 20% sucrose/PBS for cryosectioning, as previously detailed (Hou et al., 2008). Both thoracic and lumbosacral segments of cord were cryosectioned serially in the longitudinal, horizontal plane at 50 μm, and consecutively mounted onto glass slides (Superfrost Plus; Fisher Scientific) in 5 series of 5 slides each (Hou et al., 2008). The celiac ganglia were cryosectioned serially in the longitudinal plane at 20 μm, and mounted consecutively onto glass slides in 5 series of 5 slides each.

Immunohistochemistry

For anti-c-Fos, anti-choline acetyl transferase (ChAT) and anti-CD11b/C (OX-42) immunostaining, the slides with mounted longitudinal sections were thawed and pre-incubated in 0.1 M PBS containing 0.5% Triton-X and 5% normal donkey serum (Vector Laboratories, Burlingame, CA) for 1 h, followed by incubation with either goat anti-c-Fos (2 μg/mL, 1:100; Santa Cruz Biotechnology, Santa Cruz, CA), goat anti-ChAT (1:100; Millipore, Billerica, MA), or mouse anti-OX-42 (1:200; Abcam, Cambridge, MA), in the same buffer overnight at 4°C. The slides were then rinsed before applying secondary antibodies: rabbit anti-goat conjugated to FITC/Texas Red for c-Fos, or donkey anti-goat conjugated to Texas Red for ChAT (1:200; Jackson ImmunoResearch Laboratories, West Grove, PA) for 3 h at room temperature. For OX-42 immunostaining, biotinylated horse anti-mouse (1:200; Vector Laboratories) was applied overnight at 4°C, followed by incubation with streptavidin-FITC (1:200; Vector Laboratories) for 3 h at room temperature. After final rinses, all slides were cover-slipped using Vectashield mounting medium (Vector Laboratories) and sealed with nail varnish.

Quantification of c-Fos-positive cells in the spinal cord

The c-Fos-positive cells in spinal cord gray matter tissues were quantified in the same manner as the described below for the PRV-152-positive cells. In brief, serial longitudinal, horizontal sections (50 μm), corresponding to the caudal 2 cm of thoracic spinal cord segments T8–T13, and encompassing the dorso-ventral extent of the IML that contains the majority of SPN, were sampled using the Bioquant® image analysis program (Nova Prime, V6.70.10; Bioquant Image Analysis Corp., Nashville, TN). All c-Fos-positive cells within our region of interest (T8–T13 spinal cord gray matter, bilaterally) were counted, and potential over-counting was adjusted with the Abercrombie correction factor (see below).

Quantification of PRV-152-positive cells in the spinal cord and celiac ganglia

For PRV-152-positive cell quantification at 96 h post-PRV inoculation (immediately after CRD, or 96 h afterward), our region of interest again was the T8–T13 spinal cord gray matter, bilaterally, as previously detailed (Duale et al., 2009). To avoid counting the same cell twice, every other 50-μm section of the thoracic cord segments were analyzed, and thus were separated by 250 μm on each slide. This corresponded to quantifying three alternating serial sections through the IML gray matter for each spinal cord. Due to the smaller size of the celiac ganglia tissue, we analyzed six 20-μm sections within each adjacent slide series, and thus were separated by 100 μm on each slide. All quantifications were conducted in a blinded fashion with the Bioquant image analysis program, using established methods (Duale et al., 2009; Hou et al., 2008). In brief, under an Olympus BX51 fluorescence microscope (Olympus Corp., Melville, NY), live images corresponding to bilateral gray matter regions in our area of interest (T8–T13) were circumscribed at 4×magnification (1×eyepiece), and the images were captured using an Optronics digital video camera (Optronics Corp., Goleta, CA). In conjunction with Microcode II stage encoders (Boeckler Instruments, Tucson, AZ), and using a 60×oil-immersion objective (10×eyepiece), all

EGFP-positive cells within the circumscribed area through the section plane were counted. Although counting all objects within a circumscribed area is a valid and efficient method, it is prone to over-counting. To minimize over-counting, we used the correction factor first computed by Abercrombie (Abercrombie, 1946; Duale et al., 2009; Guillery, 2002; Hou et al., 2008). The photomicrographs in all figures were optimized for final production by adjusting only the brightness and contrast using Adobe Photoshop 7.0 (Adobe Systems Inc., San Jose, CA). All graphs were created with DeltaGraph 5.4 (Red Rock Software, Inc., Salt Lake City, UT).

Statistical analysis

Statistical analyses of the spinal-transected and non-transected rats were performed using Statview (SAS Institute, Cary, NC). An unpaired Student's *t*-test was used between the uninjured and injured, as well as the stimulated and non-stimulated groups. Significance throughout all experiments was set at $p < 0.05$. Data are represented as means $\pm$ standard deviation.

Results

Phenotypic characterization of PRV-152-positive cells in the thoracolumbar spinal cord

Phenotypic analysis of PRV-152-positive neurons (Fig. 1A) under fluorescent microscopy in both sham and T4-transected spinal cord tissues revealed co-localization with ChAT throughout the thoracolumbar spinal cord (Fig. 1B and C). The pattern of ChAT immunolabeling was remarkably similar in injured and in sham spinal cords, most notably in the IML. However, despite reduced PRV152-positive cell labeling in the IML after SCI, complete co-localization of GFP with ChAT-immunolabeled cells was not observed. This suggests trans-synaptic transport of PRV-GFP to second- or even third-order, non-cholinergic spinal interneurons, as indicated following PRV inoculation in the bladder of sham rats or rats with complete SCI (Im et al., 2008).

Effects of T4 spinal transection on c-Fos expression patterns in the thoracolumbar spinal cord

c-Fos expression is used as a marker to identify spinal neurons activated by different types of stimuli, including pelvic visceral distension after SCI (Hou et al., 2008; Xu et al., 2006). Qualitative assessment of c-Fos expression following intermittent CRD in 2-week-injured rats showed a marked increase throughout the dorsal-ventral extent of the IML in T4-transected (T4Tx) versus sham rats (Fig. 2A and B). Subsequent quantification revealed significantly more c-Fos-positive cells in the IML of injured than in sham rats (Fig. 2C). Notably, the animals in this experiment were not inoculated with PRV-152 due to the pronounced innate immune reaction to viral infection of the CNS.

Colorectal distension stimulation prior to pseudorabies virus inoculation

Distribution of EGFP-positive cells in spinal cord and celiac ganglion. As we reported previously (Duale et al., 2009), complete high T4Tx significantly reduces the number of PRV-152-positive cells in the thoracolumbar spinal cord, as well as in the celiac ganglia. On the contrary, noxious intermittent CRD in injured more than sham rats resulted in increased c-Fos immunoreactivity, indicative of elevated neuronal activity (Fig. 2A). To assess whether noxious intermittent CRD prior to viral injection into the kidney alters subsequent PRV-

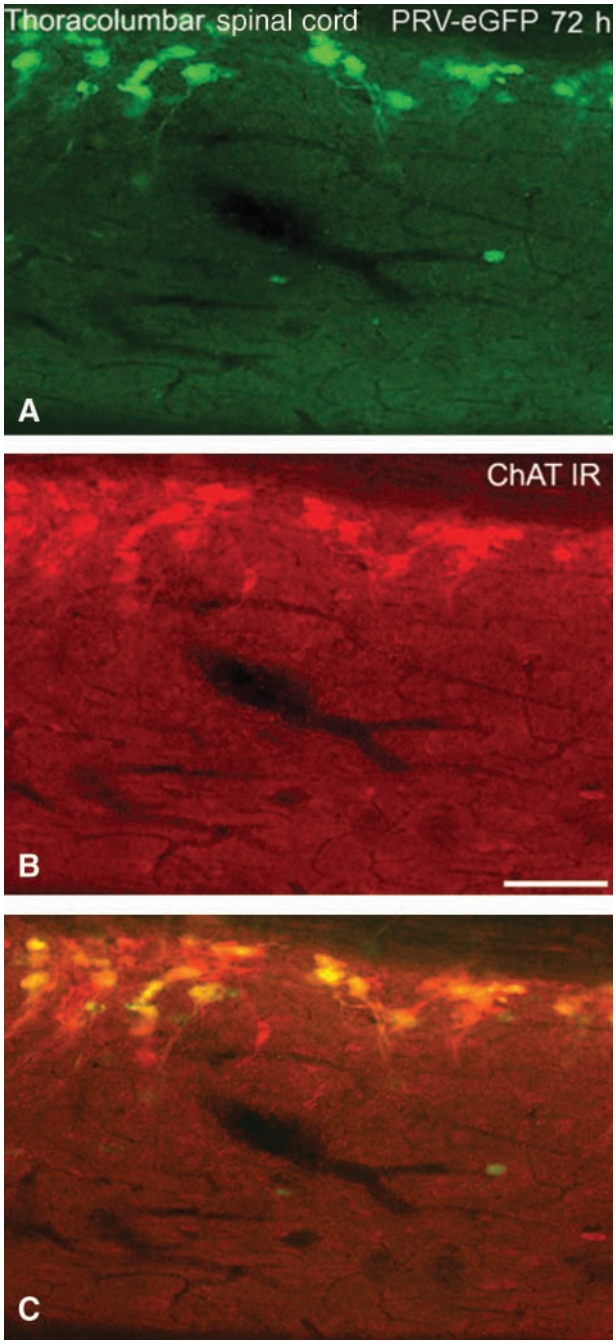

FIG. 1. Photomicrographs illustrating the co-localization of PRV-152 (EGFP)-labeled cells and choline acetyltransferase (ChAT) immunoreactivity (IR) in sympathetic preganglionic neurons (SPN) of the thoracolumbar spinal cord. (**A**) Fixed spinal cord from a naïve rat infected with PRV-152 at 72 h following inoculation of the left kidney. (**B**) ChAT-IR (red) in the same visual field. (**C**) Overlay of **A** and **B** demonstrates conspicuous co-localization of PRV-152-positive and ChAT-IR cells (scale bar = 100 μm; PRV, pseudorabies virus; EGFP, enhanced green fluorescent protein).

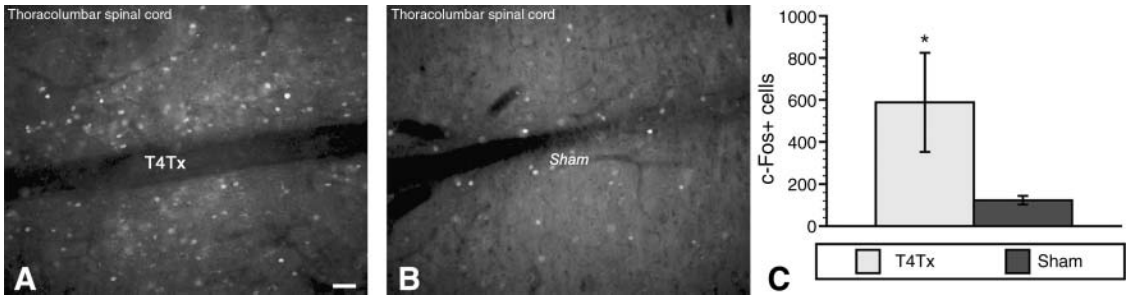

FIG. 2. Immunolabeling patterns of c-Fos-positive neurons in the intermediate gray matter (peri-central canal) of thoracolumbar spinal cord in **A**, a chronic T4-transected (T4Tx) rat, and in **B**, a sham-injured rat following 1.5 h of intermittent noxious colorectal distension (CRD). (**C**) There was a conspicuous increase in neuronal activity induced by CRD 2 weeks after T4Tx (**A** versus **B**), as reflected by significantly increased c-Fos-positive cell counts compared to stimulated sham animals (scale bar = 100 μm; bars represent means ± standard deviation; *$p < 0.05$).

152 uptake/transport in the thoracolumbar spinal cord and celiac ganglia, we subjected the test group (T4-transected + PRV + CRD; henceforth T4Tx-PRV-CRD+) to 1.5 h of intermittent CRD to stimulate increased neuronal activity. At 30 min post-CRD cessation, both the T4Tx-PRV-CRD+ test group ($n = 3$), and the T4Tx-PRV-CRD– control group, in which the balloon catheter was not inflated ($n = 3$), were injected with PRV-152 into the left kidney. Compared to the T4Tx-PRV-CRD– control group, there was a decrease in the number of PRV-152-positive cells in the thoracolumbar spinal cord of the T4Tx-PRV-CRD+ group at 96 h post-inoculation (Fig. 3A and B). Similarly, there was a marked reduction in PRV-152 + cells in the celiac ganglia (sympathetic post-ganglionic) of the T4Tx-PRV-CRD+ group versus the T4Tx-PRV-CRD– group (Fig. 3D and E). Quantitative analysis confirmed a significant ($p < 0.05$) reduction in EGFP-positive cells in both the thoracolumbar spinal cord (Fig. 3C) and celiac ganglia (Fig. 3F) of the T4Tx-PRV-CRD+ versus the T4Tx-PRV-CRD– control group.

Colorectal distension stimulation after pseudorabies virus inoculation

Distribution of EGFP-positive cells in spinal cord and celiac ganglion. We next sought to determine whether subjecting infected, injured animals to prolonged, intermittent CRD 96 h after PRV inoculation of the kidney would alter the expression and distribution of EGFP-positive cells that might otherwise be labeled too faintly to be detected by a standard epifluorescence microscope. Injured animals were again

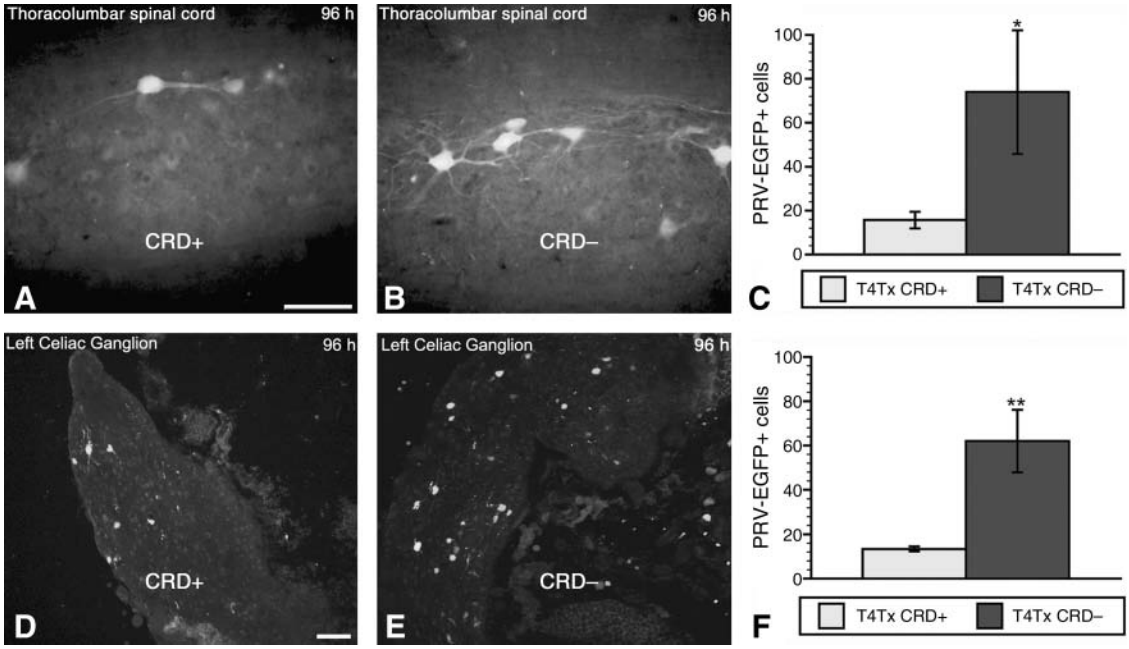

FIG. 3. Distribution patterns of PRV-152-infected neurons in the thoracolumbar spinal cord (**A** and **B**), and left celiac ganglion (**D** and **E**), of stimulated (CRD+; **A** and **D**), and non-stimulated (CRD–; **B** and **E**) rats at 2 weeks post-spinal cord injury, followed immediately by viral inoculation of the left kidney. Quantification of PRV152 + neurons at 96 h post-inoculation in both the thoracolumbar spinal cord (**C**), and left celiac ganglion (**F**), demonstrated significantly reduced PRV-152 labeling in the CRD+ injured group compared to CRD– injured rats (scale bars = 50 μm in **A** and **B**, 100 μm in **D** and **E**; bars represent means ± standard deviation; *$p < 0.05$; **$p < 0.01$; PRV, pseudorabies virus; CRD, colorectal distension).

separated into test (T4Tx-PRV-CRD+) and control (T4Tx-PRV-CRD–) groups. We found that when PRV injections were delayed by 4 days after prolonged, intermittent CRD, there were no qualitative or quantitative differences in the number and distribution of EGFP-positive cells between the test and control injured groups in the thoracolumbar spinal cord (Fig. 4A–C), or celiac ganglia (Fig. 4D–F).

Microglial phenotypes in the spinal cord after injury and noxious colorectal distension

One possible explanation for the observed reduced EGFP-PRV labeling in our stimulated (CRD+) versus non-stimulated (CRD–) paradigm may be an enhanced neuro-immune response to metabolic stress induced by prolonged, noxious stimulation. To assess whether microglia were differentially activated, we immunostained for OX-42 in spinal cord sections from the T4Tx alone, T4Tx + CRD, and sham + CRD groups (tissues from the c-Fos experiment without PRV). Compared to T4Tx alone spinal cords (Fig. 5A and D), there were marked differences in the distribution and morphologies of activated microglia in sham + CRD (Fig. 5B and E), and T4Tx + CRD (Fig. 5C and F) rats. The density of activated microglia appeared to be greater in the T4Tx group (Fig. 5D) than in the sham + CRD group (Fig. 5E). Somewhat like T4Tx alone (Fig. 5A and D), clusters of activated microglia with stout morphology and retracted processes were seen in the white matter of the T4Tx + CRD group (Fig. 5C and F). However, compared to T4Tx alone (Fig. 5D), the density of reactive microglial cells (green) in the thoracolumbar gray matter appeared greater when intermixed among c-Fos-positive cells (red) in the T4Tx + CRD group (Fig. 5F). In addition, highly reactive OX-42-positive microglial cells and their processes were often observed in close association with preganglionic neurons in the thoracolumbar spinal cord at 96 h after inoculation of the kidney with PRV-614 (Fig. 6), a PRV Bartha construct that reports via a red fluorescent protein (Banfield et al., 2003).

Discussion

Establishing a thorough characterization of injury-induced spinal cord plasticity could enable the development of treatments for debilitating secondary impairments following SCI, including autonomic dysreflexia, a potentially life-threatening hypertensive syndrome (Karlsson, 1999; Lindan et al., 1980). Genetically modified viral vectors like the PRV used in our study have greatly expanded our understanding of the intricate neural circuitry in the normal CNS (Banfield et al., 2003; Buijs et al., 2003; Card et al., 1990; Nadelhaft et al., 1992; Smith et al., 2000). Despite the important insights gained through the use of PRV, there are potential limitations to the utility of PRV as a transsynaptic marker, particularly in the complete SCI paradigm, in which the uptake of PRV by kidney-related sympathetic preganglionic neurons is markedly attenuated (Duale et al., 2009). Therefore, to better understand how cellular activity per se in the injured spinal cord influences PRV uptake, we sought to investigate whether noxious CRD, which elicits c-Fos expression in spinal rats (Hou et al., 2008), alters the attenuation of PRV uptake and transport in the injured spinal cord and sympathetic ganglia.

The temporal progression of PRV infection in the CNS after peripheral inoculation, particularly from the kidneys, has been well documented (Cano et al., 2004). We have reported that at 48–72 h post-inoculation, PRV labeling is restricted predominantly to first-order neurons in the celiac ganglia and second-order SPN, and that by 96 h the entire thoracolumbar spinal cord is labeled (Duale et al., 2009). In the

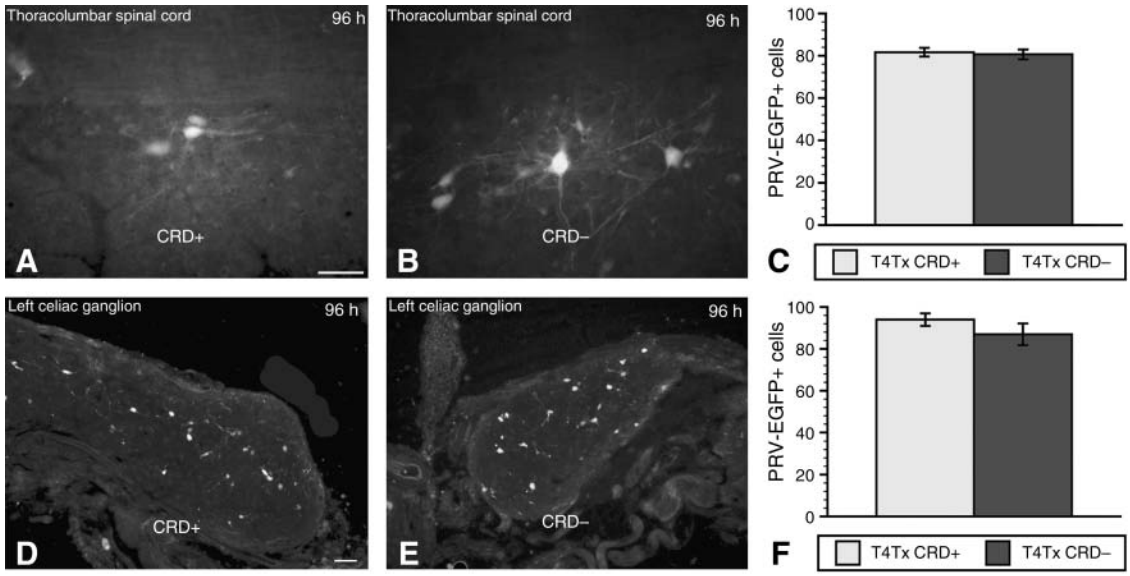

FIG. 4. Distribution patterns of PRV-152-infected neurons in the thoracolumbar spinal cord (**A** and **B**), and left celiac ganglion (**D** and **E**), of stimulated (CRD+; **A** and **D**), and non-stimulated (CRD–; **B** and **E**) rats at 2 weeks post-injury, followed 4 days later by viral injections into the left kidney. Quantification of PRV-152-positive neurons at 96 h post-inoculation in both the thoracolumbar spinal cord (**C**), and left celiac ganglion (**F**), revealed no significant alterations in PRV-152 labeling in the CRD-positive injured group compared to CRD– injured rats (scale bars = 50 μm in **A** and **B**, and 100 μm in **D** and **E**; bars represent means ± standard deviation; PRV, pseudorabies virus; CRD, colorectal distension).

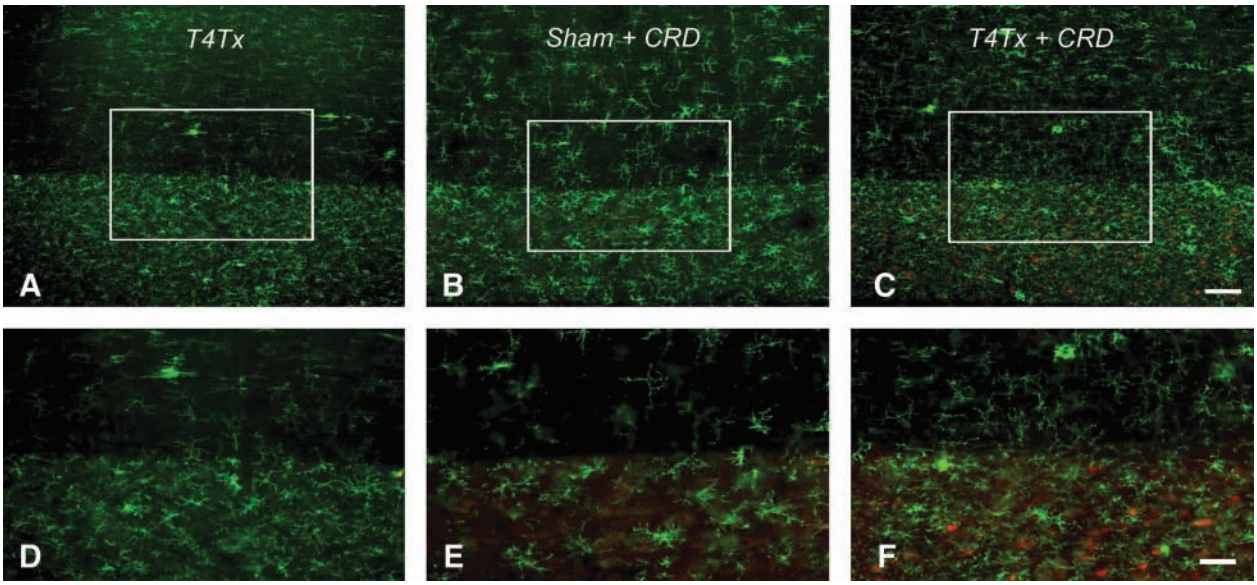

FIG. 5. Photomicrographs illustrating OX-42 immunostaining of microglia in longitudinal, horizontal sections of thoracolumbar spinal cords from 2-week-injured and sham rats immediately following prolonged, intermittent noxious colorectal distension (CRD; c-Fos experimental groups). (**A**) OX-42 labeling of a section from an animal with a T4 transection (T4Tx) but no CRD stimulation. (**B**) OX-42 labeling of a section from a sham-injured animal that was stimulated with CRD (i.e., Sham + CRD). (**C**) OX-42 labeling of a section from an animal with T4Tx and CRD stimulation (i.e., T4Tx + CRD). **A** and **D** (T4Tx) are immunostained for OX-42 alone (fluorescein isothiocyanate; FITC), whereas **B**, **C**, **E** and **F** are stained for both OX-42 (FITC) and c-Fos (Texas Red). Higher magnifications of boxed regions in **A**–**C** are shown in **D**–**F**, respectively. Somewhat similar to T4Tx alone (**D**), but unlike the sham-injured stimulated group (**E**), the injured stimulated group (**F**) exhibited dense clusters of activated microglia with stout morphology and retracted processes in the white matter (top of panels), and intermixed among c-Fos-positive cells (red) in the gray matter (scale bars = 500 μm in **A** and **B**, 100 μm in **C** and **D**).

current study, phenotypic analysis of PRV-152-positive cells in the IML revealed the majority to be cholinergic, the classical marker for SPN that play a crucial role in cardiovascular homeostasis. However, following SCI the SPN undergo distinct morphological changes (Krassioukov and Weaver, 1995), and due to loss of supraspinal modulation their activation can trigger episodic hypertensive syndromes like autonomic dysreflexia (Krassioukov and Weaver, 1996). Complete high thoracic spinal cord transection in adult rats significantly attenuates the ability of SPN to take up and transport PRV virions from the kidneys compared to sham-injured animals (Duale et al., 2009). This marked reduction in PRV uptake could be explained in part by the observed downregulation of critical PRV ligands such as glycoproteins B and C, that are essential for PRV binding and uptake. Conversely, like in our previous studies (Hou et al., 2008), we found that prolonged, intermittent CRD in our injury paradigm elicited significantly more c-Fos expression (an indirect marker for increased neuronal activity) in the thoracolumbar spinal cord compared to sham-injured animals. Using these two separate but interlinked data, we postulated that increasing neuronal activity via prolonged, intermittent CRD prior to and/or after PRV inoculation into the kidneys would augment PRV labeling in injured-stimulated (CRD+) more than in injured-non-stimulated (CRD–) rat spinal cords.

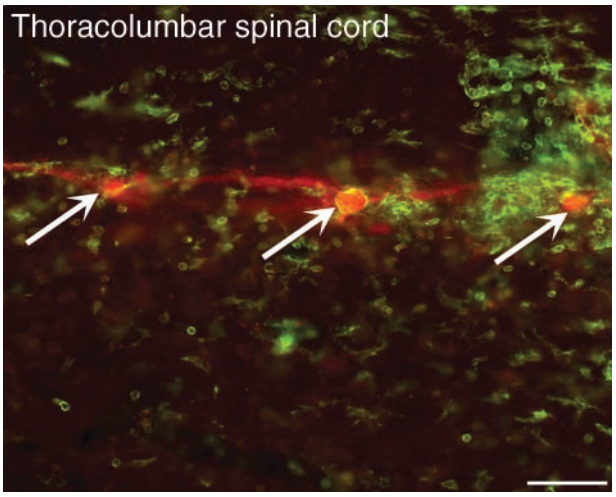

FIG. 6. Photomicrographic representation of PRV-614-positive (red) neurons (arrows), surrounded by highly reactive OX-42-positive microglial cells and their processes (green), in the thoracolumbar spinal cord at 96 h post-viral inoculation of the left kidney (scale bar = 50 μm).

Paradoxically, our results revealed a significant reduction in PRV labeling in the thoracolumbar spinal cord and celiac ganglia of injured rats when prolonged, intermittent CRD was applied just prior to PRV inoculation. Conversely, when prolonged, intermittent CRD was applied 96 h after PRV inoculation of the kidneys, we observed no qualitative or quantitative differences in the distribution of PRV-152-positive cells in the thoracolumbar spinal cord and celiac ganglia. One plausible explanation for the latter result may be that by 96 h post-inoculation, viral uptake and transport to the spinal cord and celiac ganglion were essentially complete, such that

delayed induction of intermittent CRD after inoculation did not affect the absolute number of PRV-152-positive cells.

A previous study indicated that PRV labeling in the dorsal root ganglia and spinal cord can vary across the estrous cycle following kidney inoculation (Weiss et al., 2001), with animals in diestrus demonstrating more labeled cells. It is therefore possible that a portion of the decreased PRV labeling was related to an effect on the progression of the estrous cycle rather than only elevated neuronal activity. However, the animals in this study were housed together and were inoculated in cohorts of injured and uninjured rats on multiple different days. Thus while the CRD+ and CRD– spinalized rats were examined together, the individual cohorts were tested on different days. If suppressed labeling were due to estrous-cycle differences, this should have been apparent within a given cohort. Although it seems unlikely that all animals in a given group happened to be inoculated at the same point in the cycle, the effect of estrous cycle on PRV labeling after CRD remains to be elucidated in detail, in particular since elevated estradiol has immunomodulatory functions.

We and others have documented that CRD conspicuously induces c-Fos immunolabeling in the injured spinal cord compared to sham animals (Hou et al., 2008; Landrum et al., 2002), indicating that the gentle restraint of injured or sham rats during CRD did not influence the c-Fos expression observed. Moreover, urinary bladder distention results in increased c-Fos immunolabeling in specific regions of the rostrolumbar and caudal lumbosacral spinal cord that play a role in micturition reflexes (Vizzard, 2000). The expression of c-Fos, the protein product of the immediate early gene *c-fos*, is used as a nuclear marker to identify neurons activated by different types of stimuli, including injury, neuroactive drugs, and growth factors (Sagar et al., 1988; Xu et al., 2006). The principal caveat of c-Fos immunolabeling is that it only labels cells that are activated, but not inhibited, by a stimulus. Accordingly, such cells could be motor neurons or interneurons, and since PRV labels cells transsynaptically, there is no way to differentiate them using these methods alone.

Herein we report that increased c-Fos expression induced by acute CRD is accompanied by a further, significant reduction in PRV-152-positive cellular labeling in both the spinal cord IML and celiac ganglia. It cannot be determined whether c-Fos expression was altered in neurons infected with PRV, since we did not subject PRV-inoculated spinalized rats to CRD. However, one study of the transected spinal cord indicated that PRV neither stimulates nor suppresses c-Fos expression in bladder-related spinal neurons (Im et al., 2008). Moreover, Vizzard (2000), and Im and associates (2008), studied the relationship between c-Fos expression and preganglionic neurons in the sacral parasympathetic nucleus following bladder stimulation in spinalized rat models. While we did not characterize the phenotypes of c-Fos-positive neurons, they used ChAT immunolabeling to demonstrate that approximately 75–80% of the cholinergic neurons were c-Fos-positive. They concluded that the majority of PRV-labeled c-Fos-positive neurons were bladder-specific, but that a substantial number were interneurons. Similarly, we posit that many of the c-Fos-positive neurons we observed following CRD in spinalized rats reflect colon-related interneurons.

The present findings could influence interpretation of previous studies using PRV to assess neural pathways in intact and spinal cord–injured animals (Bareyre et al., 2004; Kim et al., 2002; Lane et al., 2008; Pan et al., 2005; Yu et al., 2003), including analysis of changes in c-Fos staining after SCI (Im et al., 2008). For example, decreased numbers of neurons observed in autonomic centers after SCI may be attributed to diminished viral uptake, in addition to decreased integrity of motor neuron pathways (Kim et al., 2002). Alternatively, complete SCI has little effect on PRV transport below a lesion (Yu et al., 2003), whereas studies with incomplete lesion models do not provide insight about whether reported injury-induced alterations of neural circuitry are accompanied by attenuated PRV uptake and expression (Bareyre et al., 2004; Lane et al., 2008; Pan et al., 2005). Notably, increases in PRV-labeled spinal neurons are seen weeks to months after complete SCI following bladder inoculation, suggesting a reorganization of the spinal cord circuitry controlling the bladder after injury (Yu et al., 2003). Conversely, Im and colleagues (2008) observed no significant decline in parasympathetic spinal motor neuron labeling after PRV inoculation of the bladder in chronically-injured rats, nor were c-Fos-positive cells affected by PRV itself or by SCI. This is supported by our evidence that PRV labeling of colon-related spinal parasympathetic neurons is not affected by SCI, unlike SPN (Duale et al., 2009). Thus the significant decrease in PRV-labeled SPN weeks after SCI, coupled with the further reduction seen after acute CRD in this study, may reflect short-term cellular alterations in sympathetic function associated with these manipulations. Regarding the unaltered uptake of PRV by colon-related parasympathetic neurons after injury, an important consideration is whether SCI exclusively retards PRV expression or other host cell–viral interactions, and/or whether axonal transport alterations are specific to sympathetic circuits after SCI.

Coupled with SCI-induced downregulation of PRV-specific cell surface proteins necessary for viral uptake (Duale et al., 2009), the further reduction of PRV-152-positive cells seen in the thoracolumbar spinal cords of stimulated versus non-stimulated injured rats may stem from the "priming" of a neuroglial immune response by CRD. Accordingly, diminished neuronal activity (c-Fos expression), seen in the days after a prolonged CRD session (A.G. Rabchevsky, unpublished observation), likely restored cellular homeostasis, and consequently reduced reactive gliosis and increased PRV labeling. The evidence that PRV triggers a prompt immune response within the CNS is well documented (Denes et al., 2006; Rinaman et al., 1993). PRV infection of the CNS induces rapid activation of astrocytes, microglia, and brain macrophages (Rinaman et al., 1993), as well as infiltration of CD45-positive leukocytes (Rassnick et al., 1998). Following traumatic injury, microglial cells are rapidly targeted to regions of damage to isolate damaged neurons within hours (Nimmerjahn et al., 2005), and this swift activation is facilitated by the immediate release of high-energy purine nucleotides after metabolic stress or trauma, such as ATP, ADP, and UTP, that can activate microglial cells through P2-receptor-mediated mechanisms (Davalos et al., 2005). Therefore, intermittent CRD prior to PRV infection may increase cellular activity, and consequently, metabolic stress. The increase in neuronal c-Fos expression following acute CRD can in turn further activate surrounding microglia and/or brain macrophages to significantly limit the progression of viral infection by surrounding infected neurons, thereby isolating compromised neurons and engulfing the cellular debris after their disintegration (Fig. 6).

Alternatively, PRV uptake and transport may be compromised at the initial site of infection in the kidneys, due to either a robust immune reaction, injury-mediated degeneration of synaptic connections at the post-ganglionic level, or altered systemic physiological function. A peripheral contribution to decreased uptake is supported by significantly more reduced PRV labeling in the celiac ganglia after SCI following CRD.

While we believe that the diminished infection by PRV may be related to the activity of neurons in the IML during CRD, it is possible that the CRD triggers a cascade of events (e.g., immune responses) that have acute, and potentially long-lasting, effects on neuronal behavior, including induction of immediate early genes. Such effects would only need to be sustained for 8–12 h in order to significantly affect labeled cell numbers (i.e., cell counts are significantly lower if animals are examined at earlier time points post-infection). Thus by delaying uptake or transport, CRD may potentially have substantial effects on cell labeling. Alternatively, even a brief neural immune response may set in motion long-lasting cellular responses in the CNS, that communicates with the immune system to establish the requisite neuroendocrine regulatory system essential for maintaining homeostasis (Eskandari and Sternberg, 2002). Thus a prolonged induction of CRD may affect neural activity or immune responses for a sufficient time to interfere with viral labeling. Moreover, our findings regarding microglial activation induced by acute CRD, as well as PRV, support a direct link between the innate immune response by microglia, and their ability to become effective antigen-presenting brain macrophages (Olson and Miller, 2004).

In summary, this study provides further evidence that the efficacy of PRV uptake and transport from peripheral targets into the spinal cord, notably kidney-related neurons in the IML, is strongly influenced by complete high thoracic SCI. Moreover, noxious intermittent CRD prior to, but not after, PRV inoculation further reduces PRV labeling of both the celiac ganglia and the IML. Collectively, we speculate that SCI, coupled with noxious CRD prior to PRV inoculation into the kidneys, may induce a strong neuro-immune response involving rapid microglial activation that efficiently isolates and prevents propagation of infected spinal cord neurons, notably those that are activated by noxious peripheral stimuli. With regard to our previous findings, the more diminished viral uptake into kidney-related sympathetic circuits seen after CRD-induced neuronal activation further limits the efficacy of transgene expression in the injured spinal cord. Consequently, such findings may preclude targeting of cells (e.g., SPN) with gene therapy to promote beneficial plasticity and physiological outcome measures for the treatment of autonomic dysreflexia after complete SCI above the T6 spinal cord level.

Acknowledgements

We thank Drs. Lynn Enquist (Princeton University), Peter Strick, and Patrick Card, at the Center for Neuroanatomy with Neurotropic Viruses (CNNV; University of Pittsburgh) for providing reagents and technical expertise in the production of the PRV-152; Dr. Bruce Banfield for providing the PRV-614; and Dr. Roger Tsien (UCSD) for providing the mRFP1. This work was funded by National Institute of Neurological Disorders and Stroke (NINDS; grant R01 NS049901), Kentucky Spinal Cord Injury and Head Injury Research Trust (KSCHIRT) grant #3-11 (A.G. Rabchevsky), PVA grant #2561 (H. Duale), National Institute of Diabetes and Digestive and Kidney Diseases (NIDDK) grant R01 DK056132 (B.N. Smith), and NINDS grant P30 NS051220.

Author Disclosure Statement

No competing financial interest exist.

References

Abercrombie, M. (1946). Estimation of nuclear population from microtome sections. Anat. Rec. 94, 239–247.

Banfield, B.W., Kaufman, J.D., Randall, J.A., and Pickard, G.E. (2003). Development of pseudorabies virus strains expressing red fluorescent proteins: new tools for multisynaptic labeling applications. J. Virol. 77, 10106–10112.

Bareyre, F.M., Kerschensteiner, M., Raineteau, O., Mettenleiter, T.C., Weinmann, O., and Schwab, M.E. (2004). The injured spinal cord spontaneously forms a new intraspinal circuit in adult rats. Nat. Neurosci. 7, 269–277.

Buijs, R.M., La Fleur, S.E., Wortel, J., Van Heyningen, C., Zuiddam, L., Mettenleiter, T.C., Kalsbeek, A., Nagai, K., and Niijima, A. (2003). The suprachiasmatic nucleus balances sympathetic and parasympathetic output to peripheral organs through separate preautonomic neurons. J. Comp. Neurol. 464, 36–48.

Cameron, A.A., Smith, G.M., Randall, D.C., Brown, D.R., and Rabchevsky, A.G. (2006). Genetic manipulation of intraspinal plasticity after spinal cord injury alters the severity of autonomic dysreflexia. J. Neurosci. 26, 2923–2932.

Cano, G., Card, J.P., and Sved, A.F. (2004). Dual viral transneuronal tracing of central autonomic circuits involved in the innervation of the two kidneys in rat. J. Comp. Neurol. 471, 462–481.

Cano, G., Card, J.P., Rinaman, L., and Sved, A.F. (2000). Connections of Barrington's nucleus to the sympathetic nervous system in rats. J. Auton. Nerv. Syst. 79, 117–128.

Card, J.P., Rinaman, L., Lynn, R.B., Lee, B.H., Meade, R.P., Miselis, R.R., and Enquist, L.W. (1993). Pseudorabies virus infection of the rat central nervous system: ultrastructural characterization of viral replication, transport, and pathogenesis. J. Neurosci. 13, 2515–2539.

Card, J.P., Rinaman, L., Schwaber, J.S., Miselis, R.R., Whealy, M.E., Robbins, A.K., and Enquist, L.W. (1990). Neurotropic properties of pseudorabies virus: uptake and transneuronal passage in the rat central nervous system. J. Neurosci. 10, 1974–1994.

Ch'ng, T.H., Spear, P.G., Struyf, F., and Enquist, L.W. (2007). Glycoprotein D-independent spread of pseudorabies virus infection in cultured peripheral nervous system neurons in a compartmented system. J. Virol. 81, 10742–10757.

Davalos, D., Grutzendler, J., Yang, G., Kim, J.V., Zuo, Y., Jung, S., Littmen, D.R., Dustin, M.L., and Gan, W.B. (2005). ATP mediates rapid microglial response to local brain injury in vivo. Nat Neurosci 8, 752–758.

Denes, A., Boldogkoi, Z., Hornyak, A., Palkovits, M., and Kovacs, K.J. (2006). Attenuated pseudorabies virus-evoked rapid innate immune response in the rat brain. J. Neuroimmunol. 180, 88–103.

Duale, H., Hou, S., Derbenev, A.V., Smith, B.N., and Rabchevsky, A.G. (2009). Spinal cord injury reduces the efficacy of pseudorabies virus labeling of sympathetic preganglionic neurons. J. Neuropathol. Exp. Neurol. 68, 168–178.

Eskandari, F., and Sternberg, E.M. (2002). Neural-immune interactions in health and disease. Ann. NY Acad. Sci. 966, 20–27.

Glatzer, N.R., Hasney, C.P., Bhaskaran, M.D., and Smith, B.N. (2003). Synaptic and morphologic properties in vitro of premotor

rat nucleus tractus solitarius neurons labeled transneuronally from the stomach. J. Comp. Neurol. 464, 525–539.
Guillery, R.W. (2002). On counting and counting errors. J. Comp. Neurol. 447, 1–7.
Hadziefendic, S., and Haxhiu, M.A. (1999). CNS innervation of vagal preganglionic neurons controlling peripheral airways: a transneuronal labeling study using pseudorabies virus. J. Auton. Nerv. Syst. 76, 135–145.
Hou, S., Duale, H., and Rabchevsky, A.G. (2009). Intraspinal sprouting of unmyelinated pelvic afferents after complete spinal cord injury is correlated with autonomic dysreflexia induced by visceral pain. Neuroscience 159, 369–379.
Hou, S., Duale, H., Cameron, A.A., Abshire, S.M., Lyttle, T.S., and Rabchevsky, A.G. (2008). Plasticity of lumbosacral propriospinal neurons is associated with the development of autonomic dysreflexia after thoracic spinal cord transection. J. Comp. Neurol. 509, 382–399.
Huang, J., and Weiss, M.L. (1999). Characterization of the central cell groups regulating the kidney in the rat. Brain Res. 845, 77–91.
Huang, J., Chowhdury, S.I., and Weiss, M.L. (2002). Distribution of sympathetic preganglionic neurons innervating the kidney in the rat: PRV transneuronal tracing and serial reconstruction. Auton. Neurosci. 95, 57–70.
Im, Y.J., Hong, C.H., Jin, M.H., Lee, B.H., and Han, S.W. (2008). c-Fos expression in bladder-specific spinal neurons after spinal cord injury using pseudorabies virus. Yonsei Med. J. 49, 479–485.
Jansen, A.S., Hoffman, J.L., and Loewy, A.D. (1997). CNS sites involved in sympathetic and parasympathetic control of the pancreas: a viral tracing study. Brain Res. 766, 29–38.
Karlsson, A.K. (1999). Autonomic dysreflexia. Spinal Cord 37, 383–391.
Kim, E.S., Kim, G.M., Lu, X., Hsu, C.Y., and Xu, X.M. (2002). Neural circuitry of the adult rat central nervous system after spinal cord injury: a study using fast blue and the Bartha strain of pseudorabies virus. J. Neurotrauma 19, 787–800.
Krassioukov, A.V., and Weaver, L.C. (1996). Morphological changes in sympathetic preganglionic neurons after spinal cord injury in rats. Neuroscience 70, 211–225.
Krassioukov, A.V., and Weaver, L.C. (1995). Reflex and morphological changes in spinal preganglionic neurons after cord injury in rats. Clin. Exp. Hypertens. 17, 361–373.
Landrum, L.M., Jones, S.L., and Blair, R.W. (2002). The expression of Fos-labeled spinal neurons in response to colorectal distension is enhanced after chronic spinal cord transection in the rat. Neuroscience 110, 569–578.
Lane, M.A., White, T.E., Coutts, M.A., Jones, A.L., Sandhu, M.S., Bloom, D.C., Bolser, D.C., Yates, B.J., Fuller, D.D., and Reier, P.J. (2008). Cervical prephrenic interneurons in the normal and lesioned spinal cord of the adult rat. J. Comp. Neurol. 511, 692–709.
Lindan, R., Joiner, E., Freehafer, A.A., and Hazel, C. (1980). Incidence and clinical features of autonomic dysreflexia in patients with spinal cord injury. Paraplegia 18, 285–292.
Nadelhaft, I., Vera, P.L., Card, J.P., and Miselis, R.R. (1992). Central nervous system neurons labelled following the injection of pseudorabies virus into the rat urinary bladder. Neurosci. Lett. 143, 271–274.
Nimmerjahn, A., Kirchhoff, F., and Helmchen, F. (2005). Resting microglial cells are highly dynamic surveillants of brain parenchyma in vivo. Science 308, 1314–1318.
Olson, J.K., and Miller, S.D. (2004). Microglia initiate central nervous system innate and adaptive immune responses through multiple TLRs. J. Immunol. 173, 3916–3924.
Pan, B., Kim, E.J., and Schramm, L.P. (2005). Increased close appositions between corticospinal tract axons and spinal sympathetic neurons after spinal cord injury in rats. J. Neurotrauma 22, 1399–1410.
Pickard, G.E., Smeraski, C.A., Tomlinson, C.C., Banfield, B.W., Kaufman, J., Wilcox, C.L., Enquist, L.W., and Sollars, P.J. (2002). Intravitreal injection of the attenuated pseudorabies virus PRV Bartha results in infection of the hamster suprachiasmatic nucleus only by retrograde transsynaptic transport via autonomic circuits. J. Neurosci. 22, 2701–2710.
Rassnick, S., Enquist, L.W., Sved, A.F., and Card, J.P. (1998). Pseudorabies virus-induced leukocyte trafficking into the rat central nervous system. J. Virol. 72, 9181–9191.
Rinaman, L., Card, J.P., and Enquist, L.W. (1993). Spatiotemporal responses of astrocytes, ramified microglia, and brain macrophages to central neuronal infection with pseudorabies virus. J. Neurosci. 13, 685–702.
Sagar, S.M., Sharp, F.R., and Curran, T. (1988). Expression of c-fos protein in brain: metabolic mapping at the cellular level. Science 240, 1328–1331.
Schramm, L.P., Strack, A.M., Platt, K.B., and Loewy, A.D. (1993). Peripheral and central pathways regulating the kidney: a study using pseudorabies virus. Brain Res. 616, 251–262.
Smith, B.N., Banfield, B.W., Smeraski, C.A., Wilcox, C.L., Dudek, F.E., Enquist, L.W., and Pickard, G.E. (2000). Pseudorabies virus expressing enhanced green fluorescent protein: A tool for in vitro electrophysiological analysis of transsynaptically labeled neurons in identified central nervous system circuits. Proc. Natl. Acad. Sci. USA 97, 9264–9269.
Standish, A., Enquist, L.W., Escardo, J.A., and Schwaber, J.S. (1995). Central neuronal circuit innervating the rat heart defined by transneuronal transport of pseudorabies virus. J. Neurosci. 15, 1998–2012.
Tang, X., Neckel, N.D., and Schramm, L.P. (2004). Spinal interneurons infected by renal injection of pseudorabies virus in the rat. Brain Res. 1004, 1–7.
Vizzard, M.A. (2000). Increased expression of spinal cord Fos protein induced by bladder stimulation after spinal cord injury. Am. J. Physiol. Regul. Integr. Comp. Physiol. 279, R295–R305.
Weiss, M.L., Dobbs, M.E., MohanKumar, P.S., Chowdhury, S.I., Sawrey, K., Guevara-Guzman, R., and Huang, J. (2001). The estrous cycle affects pseudorabies virus (PRV) infection of the CNS. Brain Res. 893, 215–226.
Xu, Y., Zheng, Z., Ho, K.P., and Qian, Z. (2006). Effects of spinal cord injury on c-fos expression in hypothalamic paraventricular nucleus and supraoptic nucleus in rats. Brain Res. 1087, 175–179.
Yu, X., Xu, L., Zhang, X.D., and Cui, F.Z. (2003). Effect of spinal cord injury on urinary bladder spinal neural pathway: a retrograde transneuronal tracing study with pseudorabies virus. Urology 62, 755–759.

Address correspondence to:
Alexander G. Rabchevsky, Ph.D.
Department of Physiology
University of Kentucky
Spinal Cord & Brain Injury Research Center (SCoBIRC)
B471, Biomedical & Biological Sciences Research Building
741 South Limestone Street
Lexington, KY 40536-0509

E-mail: AGRab@uky.edu